2. Materials and methods

2.1. Mice, cell lines, and reagents

Female C57BL/6 mice (6 weeks old) were purchased from Nippon SLC (Hamamatsu, Japan), and kept under humane conditions according to the rules and regulations of our institutional committee. *Spodoptera frugiperda* (Sf-9) cells were cultured at 27 °C in BD BaculoGold Medium (Invitrogen, Carlsbad, CA). The YAC-1 mouse lymphoma cell line was obtained from the Riken Cell Bank (Wako, Saitama, Japan) and maintained in RPMI-1640 (Sigma Chemical Co., St. Louis, MO) supplemented with 10% FBS (Sigma Chemical Co.), 100 U/ml penicillin, and 100 μg/ml streptomycin (Sigma Chemical Co.). LPS was bought from Sigma Chemical Co. Synthesized CpG-A (ODN-D19) was purchased from Hokkaido System Science (Sapporo, Hokkaido, Japan). Recombinant murine GM-CSF and murine IL-4 were bought from Pepro Tech EC Ltd. (London, UK). Anti-gp64 mouse IgG, FITC-conjugated anti-mouse CD11c, CD3, and CD69, and PE-conjugated anti-mouse CD40, CD80, CD86, H-$2k^b$, MHC-II, NK 1.1, CD4, and CD8 were purchased from eBioscience (San Diego, CA) and BD Bioscience (San Diego, CA).

2.2. Purification of wild-type baculovirus

Wild-type baculovirus was purchased from BD Bioscience, multiplied on a large scale using Sf-9 insect cells, and purified as follows: culture supernatants were harvested 3–4 days after infection, and cell debris was removed by centrifugation at 3000 rpm for 5 min. The virus was pelleted by ultracentrifugation at 25,000 rpm for 60 min at 4 °C, and then resuspended in 1 ml sterile physiological saline (PSS). The infectious titer was determined by a plaque assay.

2.3. Generation of murine bone marrow-derived DCs (BMDCs)

Murine BMDCs were generated as described previously [23]. Briefly, bone-marrow cells were harvested from the tibiae and femurs of C57BL/6 mice, and were depleted of RBCs using RBC lysis buffer (Sigma Chemical Co.). Bone-marrow cells ($2.0–3.0 \times 10^7$) were cultured in a volume of 10 ml RPMI-1640 medium containing 10% FBS, 100 U/ml penicillin, 100 μg/ml streptomycin, 2 mM L-glutamine (Invitrogen), and 50 μM 2-mercaptoethanol (Invitrogen), supplemented with 20 ng/ml murine GM-CSF and 20 ng/ml murine IL-4 in a 100 mm dish. On day 3, all of the culture medium was replaced by fresh medium supplemented with murine GM-CSF and murine IL-4 at the same concentration. On day 5, one-half of the culture medium was replaced by fresh medium containing murine GM-CSF and murine IL-4. On day 7, non-adherent and loosely adherent cells were harvested, and positively selected by anti-mouse CD11c microbeads (Miltenyi Biotech, Bergisch Gladbach, Germany).

2.4. Immunofluorescence staining

BMDCs (2.0×10^6) were infected with the baculovirus at a multiplicity of infection (MOI) of 50 for 4 h. Cells were fixed with 2% paraformaldehyde for 20 min at room temperature, washed with PBS including 0.1% Tween 20, permeabilized with 0.2% Triton X/PBS for 15 min at room temperature, and then washed again. The cells were incubated with anti-gp64 mouse IgG (1:50 dilution) as a primary Ab for 1 h at room temperature, washed three times, blocked with goat serum for 15 min at room temperature, and then washed again. The cells were incubated with goat anti-mouse IgG FITC (1:300 dilution) as a secondary Ab for 1 h at room temperature, followed by three washes. Baculovirus infection was visualized using fluorescence microscopy.

2.5. PCR analysis

Total DNA was extracted from each cell with the GenElute™ mammalian genomic DNA miniprep kit (Sigma Chemical Co.), according to the manufacturer's instructions, and total DNA was used for PCR analysis. Baculovirus DNA was detected by PCR using the virus DNA specific primers 5′-CTACTAGTAAATCAGTCACACC-3′ (sense) and 5′-CCAAGTTTTTAATCTTGTACGG-3′ (antisense). The PCR amplification conditions were as follows: a denaturation step at 94 °C for 2 min, followed by 30 cycles of 94 °C for 15 s, 60 °C for 30 s, and 68 °C for 10 s (virus DNA) or 30 s (G3PDH). Each reaction was done in a volume of 25 μl with 10 ng template DNA.

2.6. Cell-viability assay

BMDCs were infected with the baculovirus at MOI values ranging from 1 to 100. After 48 h, the cells were harvested and their viability was measured by Trypan blue staining.

2.7. Flow-cytometry analysis

BMDCs (1×10^6/well) were incubated with the baculovirus at an MOI of 50, LPS (1 μg/ml), or CpG (1 μg/ml) for 48 h. PE-conjugated anti-$H2K^b$, MHC class II, CD40, CD80, or CD86, and FITC-conjugated anti-CD11c (BD Bioscience and eBioscience) mAbs were used as primary mAbs. The cells were harvested, washed, and blocked using anti-mouse CD16/32 mAb (BD Bioscience) for 10 min at 4 °C. The cells were washed and incubated with primary Abs for 1 h at 4 °C. Thereafter, the cells were washed and analyzed using FACSCalibur with the CellQuest software (BD Bioscience).

2.8. ELISA

BMDCs (1×10^6/well) were incubated with the baculovirus at an MOI of 50, LPS (1 μg/ml), or CpG (1 μg/ml) for 48 h. The culture medium was harvested, and the concentrations of mouse IFN-α, IFN-γ, IL-6, IL-10, IL-12p70, and TNF-α were measured using the respective ELISA kits (Biosource) according to the manufacturer's protocols.

2.9. Co-cultures of DC–NK cells and DC–T cells

NK cells were purified from mice spleens using the mouse NK-cell isolation kit (Miltenyi Biotech). BMDCs (5.0×10^4/well) were infected with the wild-type baculovirus at an MOI of 50, incubated for 1 h at 37 °C, and washed with PBS. NK cells (1.0×10^5/well) were then added to the culture for 18 h. $CD4^+$ and $CD8^+$ T cells were purified from mouse spleens using the mouse $CD4^+$ T cell isolation kit or the mouse $CD8^+$ T cell isolation kit (Miltenyi Biotech). BMDCs (1.0×10^4/well) were infected with the baculovirus at an MOI of 50, incubated for 1 h, and washed. Anti-TCR αβ Ab (0.5 μg/ml) was added and cultured for 24 h. The culture medium was harvested, and the concentration of IFN-γ was measured using the mouse IFN-γ ELISA kit (Biosurce) according to the manufacturer's protocol.

2.10. In vitro cytotoxicity assay

Splenic NK cells were co-cultured with baculovirus-infected BMDCs and used as effector cells. YAC-1 cells (2×10^4) were used as target cells. BMDCs were infected with the baculovirus at an MOI of 50, incubated for 1 h at 37 °C, and washed with PBS. Thereafter, BMDCs were added to the NK-cell culture at a DC/NK ratio of

Please cite this article in press as: T. Suzuki et al., Baculovirus activates murine dendritic cells and induces non-specific NK cell and T cell immune responses, Cell. Immunol. (2010), doi:10.1016/j.cellimm.2009.12.005

1:2 for 18 h. The cells were then co-cultured at E:T ratios of 10, 5, or 2.5 for 4 h, and the cytotoxicity was examined using the CytoTox 96 non-radioactive cytotoxicity assay kit (Promega, Madison, WI) according to the manufacturer's protocol.

2.11. Cell-proliferation assay

$CD4^+$ and $CD8^+$ T cells were purified from mouse spleens using the mouse $CD4^+$ T cell isolation kit or the mouse $CD8^+$ T cell isolation kit (Miltenyi Biotech). BMDCs (1.0×10^4/well) were infected with the baculovirus at an MOI of 50, incubated for 1 h, and then washed with PBS. Thereafter, $CD4^+$ T cells or $CD8^+$ T cells (1.0×10^5/well) were added and cultured for 48 h. Cell proliferation was determined using the CellTiter 96 Aqueous One Solution cell-proliferation assay kit (Promega) according to the manufacturer's protocol.

2.12. RT-PCR

BMDCs were infected with the baculovirus at an MOI of 50. After 6 h, total RNA was extracted from each cell with the GenElute™ mammalian genomic RNA kit (Sigma Chemical Co.) according to the manufacturer's instructions. RT-PCR was then performed using an RT-PCR high-plus kit (Toyobo, Osaka, Japan) according to the manufacturer's protocol. Rae-1, H60, and Qa-1 genes were detected by RT-PCR using the following specific primers: 5′-GAAGTGGGGGA ATGTTTGACACAACC-3′ (sense) and 5′-GGACCTTGAGGTTGATCTT GGCTTTTC-3′ (antisense) for Rae-1; 5′-TCTGGGCCATCAACACTGA TGAACAG-3′ (sense) and 5′-CACCAAGCGAATACCATGAATGCCA-3′ (antisense) for H60; and 5′-TCCAAAGGCACATGTGACCCATCA-3′ (sense) and 5′-GCACCATAGCTCCAAATGATGACCACA-3′ (antisense) for Qa-1. The RT-PCR amplification conditions were as follows: reverse transcription at 60 °C for 30 min and denaturation at 94 °C for 2 min, followed by 30 cycles of 94 °C for 15 s, 60 °C for 30 s, and 68 °C for 30 s. Each reaction was carried out in a volume of 25 μl with 500 ng total RNA.

2.13. Ex vivo experiments

BMDCs (1×10^6) were incubated with the baculovirus at an MOI of 50, LPS (1 μg/ml), or CpG (1 μg/ml). At 1 h after incubation, the cells were washed twice and cultured for 5 h. The cells were then harvested, washed with PSS, and suspended in 200 μl PSS. The cells were injected i.v. into five groups of mice (with three mice per group). After 6 h, the mouse splenocytes and sera were harvested. The cells were then stained with PE-conjugated anti-NK1.1 and anti-CD3, and FITC-conjugated anti-CD69, anti-CD4, and anti-CD8 Abs before FACS analysis. The serum concentration of mouse IFN-γ was measured by an ELISA. The splenocytes and target cells (YAC-1; 2×10^4) were co-cultured at E:T ratios of 100, 50, or 25 for 4 h, and the cytotoxicity was determined.

2.14. Statistical analysis

All data are presented as the means ± SD. Statistical analysis was performed using the Student's *t*-test.

3. Results

3.1. Baculovirus infectivity in BMDCs

Baculovirus infection of mouse splenic DCs induces the secretion of IFN-α and IL-12 [19]. Kitajima et al. [22] reported that a baculovirus could infect splenic DCs *in vivo*. However, it has not been clarified whether conventional DCs or plasmacytoid DCs produce these cytokines. In the current experiment, we used BMDCs because of the possibility of differentiation into only one phenotype. We investigated whether a baculovirus could infect BMDCs *in vitro*. The BMDCs were infected with the baculovirus at an MOI of 50, and harvested 4 h later. Baculovirus-infected BMDCs were detected by immunofluorescent staining using a primary Ab to the baculovirus envelope protein gp64 and a fluorescent-conjugated

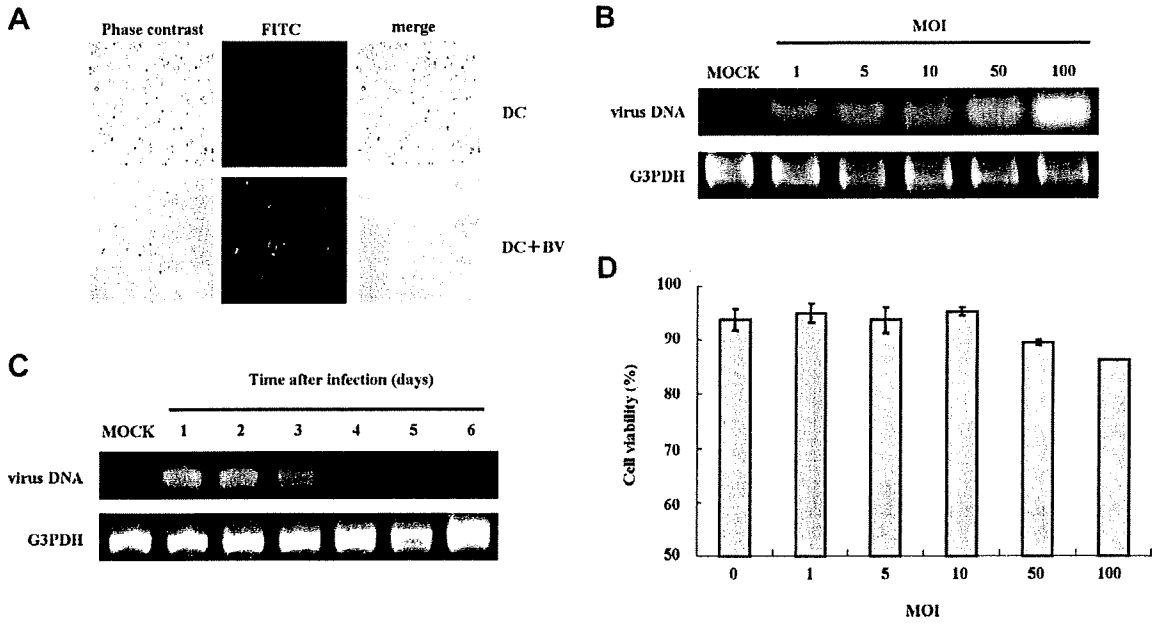

Fig. 1. Baculovirus infectivity in BMDCs. (A) BMDCs were infected with baculovirus at an MOI of 50 and cultured for 4 h. Cells were stained with anti-gp64 Ab as a primary Ab, and anti-mouse IgG FITC as a secondary Ab. Baculovirus-infected BMDCs were analyzed by fluorescence microscopy. (B) BMDCs were infected with baculovirus at MOI values ranging from 1 to 100 and cultured for 4 h. Baculovirus-infected BMDCs were detected from total DNA by PCR. (C) BMDCs were infected with baculovirus at an MOI of 50, cultured for the indicated durations, and total DNA was extracted. The baculovirus DNA was examined by PCR analysis. (D) BMDCs were infected with baculovirus at an MOI values ranging from 1 to 100 and cultured for 48 h. Cell viability was determined by Trypan blue staining. Similar results were obtained in two independent experiments.

Please cite this article in press as: T. Suzuki et al., Baculovirus activates murine dendritic cells and induces non-specific NK cell and T cell immune responses, Cell. Immunol. (2010), doi:10.1016/j.cellimm.2009.12.005

secondary Ab (Fig. 1A). The results suggested that the baculovirus could infect not only splenic DCs but also BMDCs. Next, we demonstrated the infectivity of the baculovirus to BMDCs. The BMDCs were infected with the baculovirus at MOI values ranging from 1 to 100. After 4 h, total DNA from baculovirus-infected BMDCs was collected, and the baculovirus DNA was detected by PCR. As shown in Fig. 1B, the baculovirus-infected BMDCs in a dose-dependent manner. We also investigated the degradation of the baculovirus DNA in the BMDCs. The BMDCs were infected with the baculovirus at an MOI of 50 and the total DNA was harvested every 1–6 days. The baculovirus DNA was detected by PCR using the total DNA. These results showed that the baculovirus DNA began to be degraded at 3 days post-infection, and had completely degraded 5 days later (Fig. 1C). Finally, we investigated the viability of baculovirus-infected BMDCs. The results suggested that the baculovirus did not have a significant cytopathic effect on the BMDCs (Fig. 1D).

3.2. Activation of baculovirus-infected BMDCs

Recent reports showed that mouse splenic DCs and human monocyte-derived DCs (MDDCs) produced inflammatory cytokines and IFN-α, and that MHC molecules and co-stimulation molecules were up-regulated, as a result of baculovirus infection [19,22,24,25]. In the current study, we investigated whether the baculovirus could induce BMDC activation. The BMDCs were infected with the baculovirus at an MOI of 50 as a positive control, stimulated LPS, or CpG. After 48 h, the BMDCs were analyzed for the activation markers MHC I, MHC II, CD40, CD80, and CD86 by FACS, and the cytokine levels in the culture supernatant were measured by an ELISA (Fig. 2A and B). The BMDC surface markers were strongly activated by baculovirus infection. The baculovirus-infected BMDCs showed up-regulation of MHC I, MHC II, CD40, CD80, and CD86 compared with the control BMDCs. Immature BMDCs were induced to mature by the up-regulation of MHC I and MHC II upon baculovirus infection. The baculovirus-infected BMDCs produced inflammatory cytokines (IL-6, IL12p70, and TNF-α) and IFN-α at greater levels than the control BMDCs. However, the baculovirus-infected BMDCs and control BMDCs did not produce IL-10. Furthermore, the BMDCs dose-dependently produced IL-12p70 upon baculovirus infection at MOI values ranging from 1 to 100 (Fig. 2C). These results suggested that the baculovirus induced the up-regulation of activation markers on BMDCs, as well as the production of inflammatory cytokines and IFN-α.

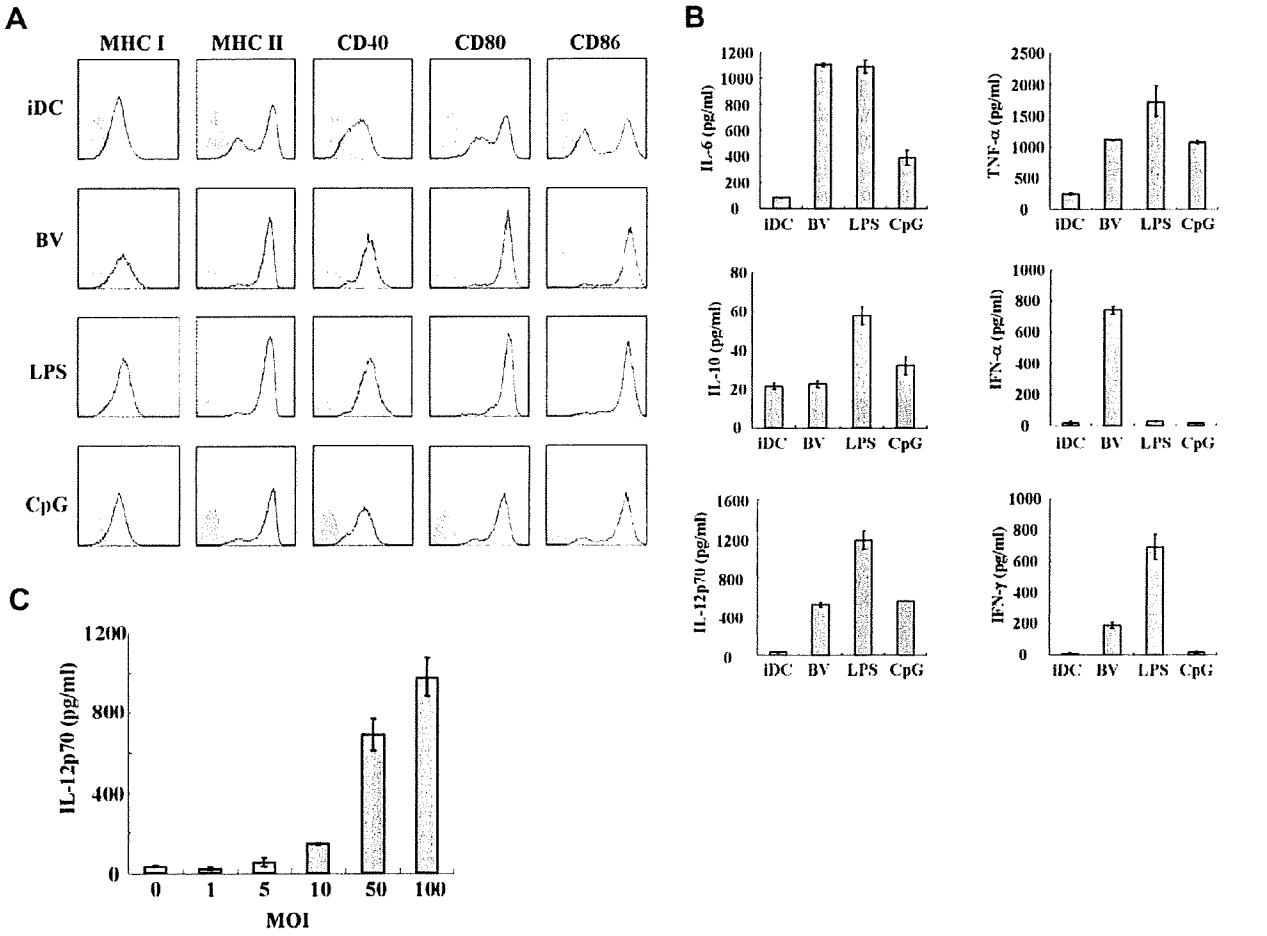

Fig. 2. Activation of baculovirus-infected BMDCs. (A) FACS analysis of cell-surface markers on baculovirus-infected BMDCs. The BMDCs were either uninfected or infected with baculovirus at an MOI of 50, or stimulated with LPS (1 μg/ml) or CpG (1 μg/ml) for 48 h. The cells were stained with the respective fluorescence-conjugated Ab, and the cell-surface markers were analyzed by FACS. Filled histograms represent the unstained cells, and black lines represent the uninfected and baculovirus-infected cells and those treated with LPS or CpG, respectively. (B) Examination of cytokine production in culture supernatants. The BMDCs were either uninfected or infected with baculovirus at an MOI of 50, or stimulated with LPS (1 μg/ml) or CpG (1 μg/ml) for 48 h, and the cytokine production was examined by an ELISA. (C) The BMDCs were infected with baculovirus at MOI values ranging from 1 to 100 and cultured for 48 h. IL12p70 production was examined by an ELISA. All data are shown as the means ± SD and done in triplicate experiments. Similar results were obtained in two independent experiments.

Please cite this article in press as: T. Suzuki et al., Baculovirus activates murine dendritic cells and induces non-specific NK cell and T cell immune responses, Cell. Immunol. (2010), doi:10.1016/j.cellimm.2009.12.005

3.3. NK-cell activation by baculovirus-infected BMDCs

Previous studies reported that NK cells showed IL-2, IFN-α, and IFN-γ production, and increased cytotoxicity, when co-cultured with cytomegalovirus-infected BMDCs or TLR ligand-stimulated BMDCs [26,27]. Here, we investigated whether the activation of NK cells could be induced by co-culturing them with baculovirus-infected BMDCs. The BMDCs were infected with baculovirus at an MOI of 50, and were co-cultured with NK cells from the mouse spleen. The early activation marker CD69 was up-regulated on NK cells co-cultured for 18 h with baculovirus-infected BMDCs in comparison to NK cells alone and uninfected BMDCs Fig. 3A). We also investigated whether NK cells showed IFN-γ production and cellular cytotoxicity against NK-sensitive YAC-1 cells (Fig. 3B and C). NK cells showed IFN-γ production and increased cytotoxicity when co-cultured with baculovirus-infected BMDCs. Andoniou et al. reported that IFN-α derived from MCMV-activated DCs as well as increased expression of NKG2D ligand in MCMV-activated DCs increases NK-cell cytotoxicity. In Fig. 2B, baculovirus-infected BMDC produced IFN-α and we suggested that BMDC-induced IFN-α up-regulates NK-cell cytotoxicity. We, therefore, evaluated whether the expression of the NKG2D ligand was up-regulated in baculovirus-infected BMDCs. The total RNA levels of the activation ligand Rae-1, H60, and the inhibitory ligand Qa-1 were examined in baculovirus-infected BMDCs by RT-PCR (Fig. 3D). The expression of H60, but not Rae-1 and Qa-1, was increased by baculovirus infection. IFN-γ production from NK cells required IL-12 and IL-18 production from activated DCs [26]. In this regard, we investigated whether BMDCs produce IL-18 upon baculovirus infection; however, we could not detect any obvious increase in IL-18 production induced by baculovirus infection (*Supplementary* Figure S1). These results suggested that NK-cell activation was induced when the cells were co-cultured with baculovirus-infected BMDCs. We predicted that NK cells that were activated by baculovirus-infected BMDCs up-regulated activation markers and produced cytokines.

3.4. Baculovirus-infected BMDCs induce T cell activation

As shown in Fig. 3, we compared the immune response between baculovirus-infected BMDCs and NK cells. We then compared the immune responses between baculovirus-infected BMDCs and T cells ($CD4^+$ and $CD8^+$ T cells). The BMDCs were infected with the baculovirus at an MOI of 50, and were co-cultured with T cells from the mouse spleen. The CD69 expression was up-regulated on T cells co-cultured with baculovirus-infected BMDCs for 18 h in comparison with T cells alone and uninfected BMDCs (Fig. 4A). In particular, the CD69 expression increased on $CD8^+$ T cells more than on $CD4^+$ cells. NK cells produced IFN-γ when co-cultured with baculovirus-infected BMDCs (Fig. 3B), whereas T cells did not (*Sup-*

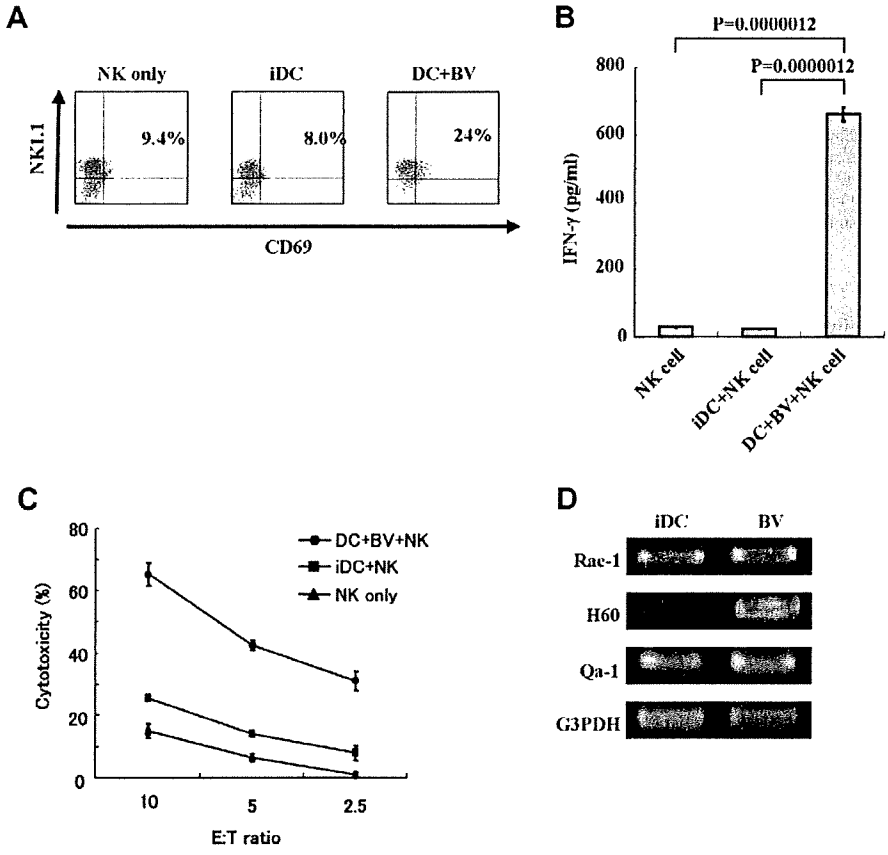

Fig. 3. Induction of NK-cell activation by baculovirus-infected BMDCs. (A) FACS analysis of CD69 expression on NK cells co-cultured with baculovirus-infected BMDCs. BMDCs were either uninfected or infected with wild-type baculovirus at an MOI of 50, and then mouse NK cells separated from spleens were added and cultured for 18 h. CD69 expression on NK cells was analyzed by FACS. (B) Examination of IFN-γ production by mouse NK cells. BMDCs were either uninfected or infected with wild-type baculovirus at an MOI of 50, and then mouse NK cells separated from spleens were added and cultured for 18 h. IFN-γ was examined by an ELISA in DC/NK co-culture supernatants. (C) Cytotoxicity assay of NK cells co-cultured with BMDC. The BMDCs were either uninfected or infected with wild-type baculovirus at an MOI of 50, and then mouse NK cells separated from spleens were added together with YAC-1 target cells at the E:T ratio indicated. After 18 h incubation, cytotoxic activity against YAC-1 was analyzed by a cytotoxicity assay kit. (D) Detection of NKG2D ligand by baculovirus-infected BMDCs. The BMDCs were either uninfected or infected with wild-type baculovirus at an MOI of 50 and cultured for 6 h. Baculovirus-infected BMDCs were detected from total RNA by RT-PCR using NKG2D ligand-specific primers. All data are shown as the means ± SD and done in triplicate experiments. Statistical analysis was performed using the Student's *t*-test. Similar results were obtained in two independent experiments.

Please cite this article in press as: T. Suzuki et al., Baculovirus activates murine dendritic cells and induces non-specific NK cell and T cell immune responses, Cell. Immunol. (2010), doi:10.1016/j.cellimm.2009.12.005

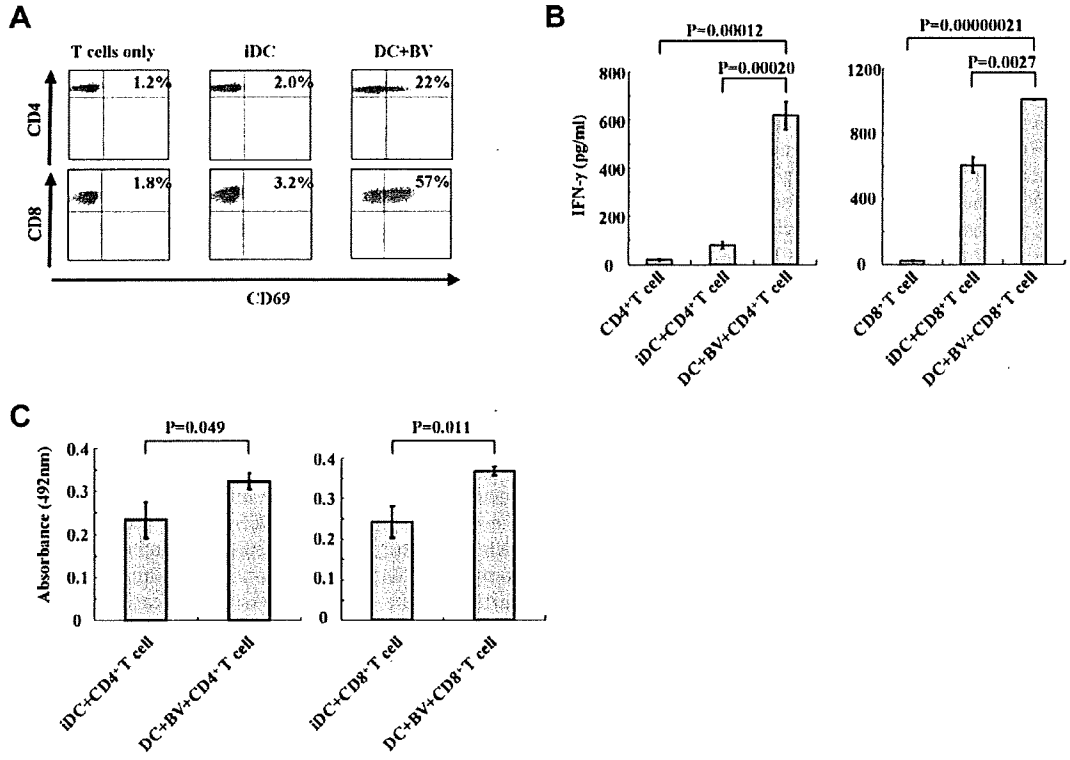

Fig. 4. Induction of T cell activation by baculovirus-infected BMDCs. (A) FACS analysis of CD69 expression on T cells co-cultured with baculovirus-infected BMDCs. BMDCs were either uninfected or infected with wild-type baculovirus at an MOI of 50, and then mouse T cells separated from spleens were added and cultured for 18 h. CD69 expression on T cells was analyzed by FACS. (B) IFN-γ production by mouse T cells. BMDCs were either uninfected or infected with wild-type baculovirus at an MOI of 50, and then mouse T cells separated from spleens and anti-TCR αβ Ab (0.5 μg/ml) were added, and cultured for 24 h. IFN-γ expression was examined by an ELISA in DC/T cell co-culture supernatants. (C) Analysis of T cell proliferation. The BMDCs were either uninfected or infected with wild-type baculovirus at an MOI of 50, and then purified mouse $CD4^+$ and $CD8^+$ T cells were added and co-cultured for 48 h. T cell proliferation was investigated using a proliferation kit. All data are shown as the means ± SD and done in triplicate experiments. Statistical analysis was performed using the Student's *t*-test. Similar results were obtained in two independent experiments.

plementary Figure S3). We investigated whether T cells produced IFN-γ after TCR stimulation using anti-TCR αβ Ab. TCR-stimulated T cells produced IFN-γ when co-cultured with baculovirus-infected BMDCs, but failed to do so when co-cultured with unstimulated BMDCs or T cells alone (Fig. 4B). T cells proliferated when co-cultured with baculovirus-infected BMDCs (Fig. 4C). These results suggested that not only NK cells but also T cells were activated by baculovirus-infected BMDCs.

3.5. Immune activation of baculovirus-infected BMDCs ex vivo

The baculovirus strongly induced the activation of BMDCs, which in turn induced the activation of NK cells and T cells *in vitro*. Here, we investigated whether baculovirus-infected BMDCs induced the activation of NK cells and T cells *ex vivo*. The BMDCs were either stimulated with the baculovirus at an MOI of 50, LPS, or CpG, or were left unstimulated. After 6 h, the stimulated BMDCs were injected i.v. into syngeneic mice, and the CD69 levels were analyzed on splenic NK cells and T cells. We also evaluated the splenocyte cytotoxicity and determined the serum IFN-γ levels. The CD69 expression on NK cells and T cells was up-regulated approximately 8-10-fold by inoculation with baculovirus-infected BMDCs compared with inoculation by other stimulated BMDCs (Fig. 5A). Increased splenocyte cytotoxicity and IFN-γ production were induced by inoculation with baculovirus-infected BMDCs (Fig. 5B and C). These results suggested that baculovirus-infected BMDCs induced the activation of splenic NK and T cells *in vivo*, similar to the results reported *in vitro*.

4. Discussion

Viral vectors derived from baculovirus are commonly used as tools for producing proteins in insect cells. Baculovirus transfer vectors have also shown promise in the development of vaccines. Baculovirus is well suited to gene-therapy applications due to its low cytotoxicity in mammalian cells even at high MOIs, its inherent inability to replicate in mammalian cells, and the absence of pre-existing Abs against baculoviruses in animals. We previously reported that baculoviruses could infect DCs and B cells more potently than other immune cells, and induced the up-regulation of activation markers on DCs [22]. However, the exact mechanisms of immune activation, such as DC-induced cytokine production, and the relationship between DCs and other immune cells are still not fully understood. Here we showed that a baculovirus induced the activation of BMDCs, and that baculovirus-infected BMDCs activated NK cells and T cells more effectively than LPS-stimulated or CpG-stimulated BMDCs.

The current study demonstrated that the immune responses of DCs were induced by baculovirus infection. Initially, we investigated whether the baculovirus could infect BMDCs *in vitro*. Our results showed that the BMDCs could be infected at an MOI as low as 1 (Fig. 1A and B). Other workers have reported that baculoviruses can also infect MDDCs [25], and that foreign genes are expressed with low efficiency after recombinant baculovirus vector infection of BMDCs [15]. We previously showed that the viral genome was degraded at 5–6 days after infection in various cell lines [28]. In the current study, the baculovirus genome was degraded 5 days

Please cite this article in press as: T. Suzuki et al., Baculovirus activates murine dendritic cells and induces non-specific NK cell and T cell immune responses, Cell. Immunol. (2010), doi:10.1016/j.cellimm.2009.12.005

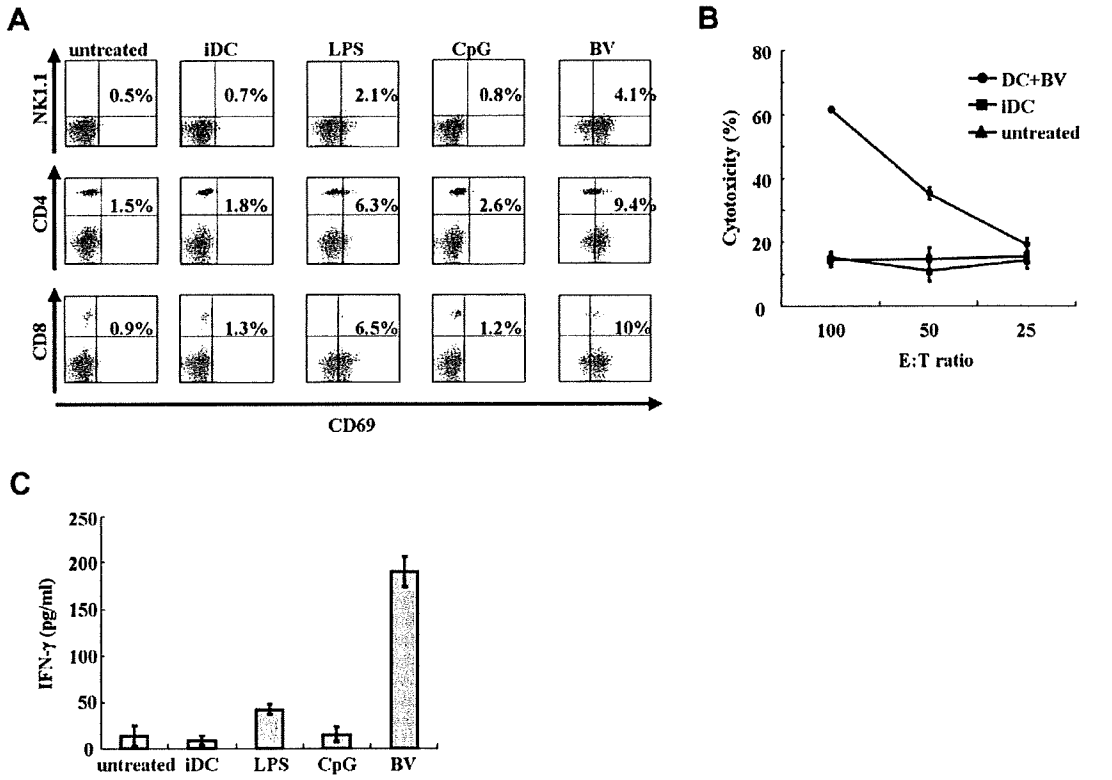

Fig. 5. Induction of NK-cell and T cell activation by baculovirus-infected BMDCs *ex vivo*. (A) Analysis of the expression of activation marker CD69 by NK cells and T cells in the mouse spleen. The BMDCs were either uninfected or infected with wild-type baculovirus at an MOI of 50, or stimulated with LPS (1 μg/ml) or CpG (1 μg/ml) and incubated for 6 h. Activated BMDCs as well as control BMDCs were inoculated (i.v.) into mice, and after 6 h the splenocytes were collected for FACS analysis of activation marker CD69. (B) Cytotoxicity assay of mouse splenocytes with or without inoculation of the control or baculovirus-activated BMDCs. The BMDCs were either uninfected or infected with wild-type baculovirus at an MOI of 50 and cultured for 6 h. Each type of BMDC was inoculated (i.v.) into mice, and after 6 h the splenocytes were collected and mixed with the YAC-1 target cells at the E:T ratio described. Cytotoxic activity was measured by a cytotoxicity assay kit. (X) Measurement of IFN-γ production from serum. The BMDCs were either uninfected or infected with wild-type baculovirus at an MOI of 50, or stimulated with LPS (1 μg/ml) or CpG (1 μg/ml) and incubated for 6 h. Activated BMDCs and control BMDCs were inoculated (i.v.) into mice, and after 6 h the serum was harvested and IFN-γ expression was measured by an ELISA. All data are shown as the means ± SD and done in triplicate experiments. Similar results were obtained in two independent experiments.

after infection in the BMDCs (Fig. 1C). The cytotoxicity due to the baculovirus infection was low even at higher MOIs (Fig. 1D). Previous studies have reported on the activation of DCs by baculovirus infection *in vitro* and *in vivo*. Baculovirus-infected MDDCs were shown to express cell-surface markers of activation and to produce TNF-α [25]. Mouse splenic DCs were also reported to express activated cell-surface markers and to produce cytokines upon baculovirus inoculation [22,24]. Our current results showed that BMDCs expressed activated cell-surface markers and produced inflammatory cytokines and IFNs due to baculovirus infection, but did not produce IL-10 (Fig. 2A–C). These findings suggested that the baculovirus could induce cellular immunity more potently than humoral immunity. NK cells produce IFN-γ through IL-12 and IL-18, secreted by activated DCs, and NK-cell cytotoxicity is increased through IFN-α and up-regulated NKG2D ligand expression by activated DCs [26]. We examined the production of IL-18 from baculovirus-infected BMDCs. However, we could not detect IL-18 production (*Supplementary* Figure S1), which was consistent with previously published reports [26]. Andoniou and coworkers suggested that IL-18 production by DCs might be restricted to the synaptic cleft [26,29]. Other authors reported that the production of IFN-γ by NK cells requires the formation of a synapse leading to IL-12 polarization in the DCs [30]. NK cells produced IFN-γ when co-cultured with baculovirus-infected BMDCs (Fig. 3B). As shown in Figs. 2A and 3B, it appeared that baculovirus-infected BMDCs produced IL-12 and NK cells produced IFN-γ. Gerosa et al. [31] reported that the expression of the early activation marker CD69 on NK cells was up-regulated when they were co-cultured with TLR ligand-stimulated DCs. The expression of CD69 required IFN-α and IFN-β secretion by DCs, and direct interaction between DCs and NK cells. We confirmed that CD69 expression was up-regulated on NK cells by baculovirus-infected BMDCs (Fig. 3A), and that NK-cell cytotoxicity was also increased (Fig. 3C). The NKG2D ligand H60 mRNA was up-regulated by baculovirus-infected BMDCs (Fig. 3D). Andoniou et al. [26] suggested that weak expression of the NKG2D ligand on mouse cytomegalovirus (MCMV)-infected BMDCs might have been sufficient to activate NK-cell cytotoxicity. Next, we investigated the relationships between baculovirus-infected BMDCs and $CD4^+$ and $CD8^+$ T cells. We confirmed that CD69 expression was up-regulated on T cells by baculovirus-infected BMDCs (Fig. 4A), and that T cell proliferation was also increased (Fig. 4C), although the T cells did not produce IFN-γ (*Supplementary* Figure S2). Feili-Hariri et al. [32] demonstrated IFN-γ production by T cells that were stimulated with anti-TCR αβ Ab. We also demonstrated that baculovirus-infected BMDCs induced IFN-γ production by T cells upon stimulation with anti-TCR αβ Ab. These results suggested that T cells produced IFN-γ when co-cultured with baculovirus-infected BMDCs (Fig. 4B). By contrast, the controls without anti-TCR αβ Ab showed no significant effects. Finally, we investigated whether baculovirus-infected BMDCs induced the activation of NK cells and T cells *ex vivo* as well as *in vitro*. Mouse splenic NK cells did not show CD69 activation in response to subcutaneous injection of BMDCs (*Supplementary* Figure S3). Eggert and coworkers reported that DCs accumulated in

Please cite this article in press as: T. Suzuki et al., Baculovirus activates murine dendritic cells and induces non-specific NK cell and T cell immune responses, Cell. Immunol. (2010), doi:10.1016/j.cellimm.2009.12.005

the spleen more than in other organs in intravenously injected mice [33]. Unstimulated BMDCs, baculovirus-infected BMDCs, and LPS-stimulated or CpG-stimulated BMDCs were injected intravenously into respective mice, and the expression of CD69 on NK cells and T cells was examined by FACS analysis. The results suggested that the CD69 expression on splenic NK cells and T cells was up-regulated by baculovirus-infected BMDCs more than the controls (Fig. 5A), and the splenocyte cytotoxicity also increased (Fig. 5B). The presence of IFN-γ in the serum was confirmed in mice injected with baculovirus-infected BMDCs (Fig. 5C). These results indicated that baculovirus-infected BMDCs induced the non-specific activation of splenic NK cells and T cells *ex vivo*, the same as *in vitro* results. We have previously shown that wild-type baculovirus induces anti-tumor acquired immunity against challenged tumor cells in the form of increased CTL activity and tumor-specific antibody production [34].

Although specific immune responses against viral infections and tumors are the essential arm of immunity, non-specific immune responses are also reported to be an important factor in control of viral infections such as HIV infection. The presence of functional HIV-specific CTL responses and $CD4^+$ T helper responses do not protect against progression to AIDS in the chronic phase of HIV infection [35]. Recently, it has been apparent that a $CD8^+$ T cell-inducing vaccine has failed in a phase IIB clinical trial. The presence of high numbers of cytokine-producing HIV-specific $CD8^+$ T cells does not guarantee a better clinical outcome [36]. Taking these reports into account, we emphasized to examine non-specific immune responses induced by wild-type baculovirus in this report.

In conclusion, the baculovirus induced the expression of activation markers on DCs, and the production of inflammatory cytokines (IL-6, IL-12p70, and TNF-α) and IFN-α. Furthermore, the baculovirus-infected BMDCs induced stronger activation of NK cells and T cells than LPS-stimulated or CpG-stimulated BMDCs. The NK cells showed IFN-γ production, up-regulated cytotoxicity, and CD69 expression. The T cells showed IFN-γ production, up-regulated proliferation, and increased CD69 expression. Baculovirus-infected BMDCs might therefore be a useful tool as an immunotherapy in the treatment of viral infections and malignancies to be used in association with present therapies to achieve most effective results.

Acknowledgments

We thank Y. Mori, S. Yanase, and Y. Kasai for excellent technical assistance. This work was supported, in part, by a Grant-in-Aid for High Technology Research from the Ministry of Education, Science, Sports, and Culture, Japan, and by a grant from the Research and Development Program for New Bio-industry Initiatives from the Ministry of Agriculture and Forestry, and Fisheries of Japan.

Appendix A. Supplementary data

Supplementary data associated with this article can be found, in the online version, at doi:10.1016/j.cellimm.2009.12.005.

References

[1] A. Huser, C. Hofmann, Baculovirus vectors: novel mammalian cell gene-delivery vehicles and their applications, Am. J. Pharmacogenomics 3 (2003) 53–63.
[2] I. Berger, D.J. Fitzgerald, T.J. Richmond, Baculovirus expression system for heterologous multiprotein complexes, Nat. Biotechnol. 22 (2004) 1583–1587.
[3] Y. Matsuura, R.D. Possee, H.A. Overton, D.H. Bishop, Baculovirus expression vectors: the requirements for high level expression of proteins, including glycoproteins, J. Gen. Virol. 68 (1987) 1233–1250.
[4] L.M. Stewart, M. Hirst, M. López-Ferber, A.T. Merryweather, P.J. Cayley, R.D. Possee, Construction of an improved baculovirus insecticide containing an insect-specific toxin gene, Nature 352 (1991) 85–88.
[5] S.C. Jennifer, L.H. Mark, W. Trevor, S.H. Rosemary, G. David, M.G. Bernadette, M.C. Timothy, D.P. Robert, P.J. Cayley, H.L. David, Field trial of a genetically improved baculovirus insecticide, Nature 370 (1994) 138–140.
[6] S.U. Song, F.M. Boyce, Combination treatment for osteosarcoma with baculoviral vector mediated gene therapy (p53) and chemotherapy (adriamycin), Exp. Mol. Med. 33 (2001) 46–53.
[7] S. Yla-Herttuala, K. Alitalo, Gene transfer as a tool to induce therapeutic vascular growth, Nat. Med. 9 (2003) 694–701.
[8] S.Y. Tjia, G.M. zu Altenschildesche, W. Doerfler, *Autographa californica nuclear polyhedrosis virus* (AcNPV) DNA does not persist in mass cultures of mammalian cells, Virology 125 (1983) 107–117.
[9] J.P. Condreay, S.M. Witherspoon, W.C. Clay, T.A. Kost, Transient and stable gene expression in mammalian cells transduced with a recombinant baculovirus vector, Proc. Natl. Acad. Sci. USA 96 (1999) 127–132.
[10] H. Tani, M. Nishijima, H. Ushijima, T. Miyamura, Y. Matsuura, Characterization of cell-surface determinants important for baculovirus infection, Virology 279 (2001) 343–353.
[11] T. Cheng, C.Y. Xu, Y.B. Wang, M. Chen, T. Wu, J. Zhang, N.S. Xia, A rapid and efficient method to express target genes in mammalian cells by baculovirus, World J. Gastroenterol. 10 (2004) 1612–1618.
[12] T. Abe, H. Takahashi, H. Hamazaki, N. Miyano-Kurosaki, Y. Matsuura, H. Takaku, Baculovirus induces an innate immune response and confers protection from lethal influenza virus infection in mice, J. Immunol. 171 (2003) 1133–1139.
[13] L. Liqun, L. Yu, J. Kwang, Baculovirus surface-displayed hemagglutinin of H5N1 influenza virus sustains its authentic cleavage, hemagglutination activity, and antigenicity, Biochem. Biophys. Res. Commun. 358 (2007) 404–409.
[14] Y. Ding-Gang, C. Yao-Chi, L. Yiu-Kay, L. Chia-Wei, L. Hung-Jen, H. Yu-Chen, Avian influenza virus envelope: cytoplasmic domain affects virus properties and vaccine potential, Mol. Ther. 15 (2007) 989–996.
[15] R. Strauss, A. Hüser, S. Ni, S. Tuve, N. Kiviat, P.S. Sow, C. Hofmann, A. Lieber, Baculovirus-based vaccination vectors allow for efficient induction of immune responses against *Plasmodium falciparum* circumsporozoite protein, Mol. Ther. 15 (2007) 193–202.
[16] H. Fan, Y. Pan, L. Fang, D. Wang, S. Wang, Y. Jiang, H. Chen, S. Xiao, Construction and immunogenicity of recombinant pseudotype baculovirus expressing the capsid protein of porcine circovirus type 2 in mice, J. Virol. Methods 150 (2008) 21–26.
[17] A. Facciabene, L. Aurisicchio, N. La Monica, Baculovirus vectors elicit antigen-specific immune responses in mice, J. Virol. 78 (2004) 8663–8672.
[18] L. Shan, L. Wang, J. Yin, P. Zhong, J. Zhong, An OriP/EBNA-1-based baculovirus vector with prolonged and enhanced transgene expression, J. Gene Med. 8 (2006) 1400–1406.
[19] T. Abe, H. Hemmi, K. Moriishi, S. Tamura, H. Takaku, S. Akira, Y. Matsuura, Involvement of the toll-like receptor 9 signaling pathway in the induction of innate immunity by baculovirus, J. Virol. 79 (2005) 2847–2858.
[20] J. Banchereau, R.M. Steinman, Dendritic cells and the control of immunity, Nature 392 (1998) 245–252.
[21] M.A. Cooper, T.A. Fehniger, M.A. Caligiuri, The biology of human natural killer-cell subsets, Trends Immunol. 22 (2001) 633–640.
[22] M. Kitajima, T. Abe, N. Miyano-Kurosaki, M. Taniguchi, T. Nakayama, H. Takaku, Induction of natural killer cell-dependent antitumor immunity by the *Autographa californica* multiple nuclear polyhedrosis virus, Mol. Ther. 16 (2008) 261–268.
[23] K. Inaba, M. Inaba, N. Romani, H. Aya, M. Deguchi, S. Ikehara, Generation of large numbers of dendritic cells from mouse bone marrow cultures supplemented with granulocyte/macrophage colony-stimulating factor, J. Exp. Med. 176 (1992) 1693–1702.
[24] S. Hervas-Stubbs, P. Rueda, L. Lopez, C. Leclerc, Insect baculoviruses strongly potentiate adaptive immune responses by inducing type I IFN, J. Immunol. 178 (2007) 2361–2369.
[25] A. Schütz, N. Scheller, T. Breinig, A. Meyerhans, The *Autographa californica* nuclear polyhedrosis virus AcNPV induces functional maturation of human monocyte-derived dendritic cells, Vaccine 24 (2006) 7190–7196.
[26] C.E. Andoniou, S.L. van Dommelen, V. Voigt, D.M. Andrews, G. Brizard, C. Asselin-Paturel, T. Delale, K.J. Stacey, G. Trinchieri, M.A. Degli-Esposti, Interaction between conventional dendritic cells and natural killer cells is integral to the activation of effective antiviral immunity, Nat. Immunol. 6 (2005) 1011–1019.
[27] I. Zanoni, M. Foti, P. Ricciardi-Castagnoli, F. Granucci, TLR-dependent activation stimuli associated with Th1 responses confer NK cell stimulatory capacity to mouse dendritic cells, J. Immunol. 175 (2005) 286–292.
[28] M. Kitajima, H. Hamazaki, N. Miyano-Kurosaki, H. Takaku, Characterization of baculovirus *Autographa californica* multiple nuclear polyhedrosis virus infection in mammalian cells, Biochem. Biophys. Res. Commun. 343 (2006) 378–384.
[29] C. Semino, G. Angelini, A. Poggi, A. Rubartelli, NK/iDC interaction results in IL-18 secretion by DCs at the synaptic cleft followed by NK cell activation and release of the DC maturation factor HMGB1, Blood 106 (2005) 609–616.
[30] C. Borg, A. Jalil, D. Laderach, K. Maruyama, H. Wakasugi, S. Charrier, B. Ryffel, A. Cambi, C. Figdor, W. Vainchenker, A. Galy, A. Caignard, L. Zitvogel, NK cell activation by dendritic cells (DCs) requires the formation of a synapse leading to IL-12 polarization in DCs, Blood 104 (2004) 3267–3275.

Please cite this article in press as: T. Suzuki et al., Baculovirus activates murine dendritic cells and induces non-specific NK cell and T cell immune responses, Cell. Immunol. (2010), doi:10.1016/j.cellimm.2009.12.005

[31] F. Gerosa, A. Gobbi, P. Zorzi, S. Burg, F. Briere, G. Carra, G. Trinchieri, The reciprocal interaction of NK cells with plasmacytoid or myeloid dendritic cells profoundly affects innate resistance functions, J. Immunol. 174 (2005) 727–734.
[32] M. Feili-Hariri, D.H. Falkner, P.A. Morel, Polarization of naive T cells into Th1 or Th2 by distinct cytokine-driven murine dendritic cell populations: implications for immunotherapy, J. Leukoc. Biol. 78 (2005) 656–664.
[33] A.A. Eggert, M.W. Schreurs, O.C. Boerman, W. Oyen, A.J. de Boer, C.J. Punt, C.G. Figdor, G.J. Adema, Biodistribution and vaccine efficiency of murine dendritic cells are dependent on the route of administration, Cancer Res. 59 (1999) 3340–3345.
[34] M. Kitajima, H. Takaku, Induction of antitumor acquired immunity by baculovirus *Autographa californica* multiple nuclear polyhedrosis virus infection in mice, Clin. Vaccine Immunol. 15 (2008) 376–378.
[35] C.A. Jansen, D. van Baarle, F. Miedema, HIV-specific $CD4^+$ T cells and viremia: who's in control?, Trends Immunol 27 (2006) 119–124.
[36] I.M. Schellens, J.A. Borghans, C.A. Jansen, I.M. De Cuyper, R.B. Geskus, D. van Baarle, F. Miedema, Abundance of early functional HIV-specific $CD8^+$ T cells does not predict AIDS-free survival time, PLoS ONE 3 (2008) e2745.

Please cite this article in press as: T. Suzuki et al., Baculovirus activates murine dendritic cells and induces non-specific NK cell and T cell immune responses, Cell. Immunol. (2010), doi:10.1016/j.cellimm.2009.12.005

Antiviral Chemistry & Chemotherapy 2010 20: in press (doi: 10.3851/IMPxx)

Original article

Combination therapy for hepatitis C virus with heat-shock protein 90 inhibitor 17-AAG and proteasome inhibitor MG132

*Saneyuki Ujino[1], Saori Yamaguchi[1], Kunitada Shimotohno[2,3] and Hiroshi Takaku[1,2,4]**

[1]Department of Life and Environmental Sciences, Chiba Institute of Technology, Tsudanuma, Narashino, Chiba, Japan
[2]Research Institute, Chiba Institute of Technology, Tsudanuma, Narashino, Chiba, Japan
[3]Center of Integrated Medical Research, School of Medicine, Keio University, Tokyo, Japan
[4]High Technology Research Center, Chiba Institute of Technology, Tsudanuma, Narashino, Chiba, Japan

*Corresponding author: e-mail: hiroshi.takaku@it-chiba.ac.jp

Background: Hepatitis C virus (HCV) infection is a major cause of chronic liver disease. Here, we report a new and effective strategy for inhibiting HCV replication using an inhibitor of heat-shock protein 90, 17-AAG (17-allylamino-17demethoxygeldanamycin), and a proteasome inhibitor, MG132.

Methods: To explore the virological basis of combination therapy, we analysed the effects of 17-AAG and MG132, singly and in combination on HCV replication in an HCV replicon cell system.

Results: In HCV replicon cells, HCV RNA replication was suppressed by 17-AAG in a dose-dependent manner. As shown in the present study, the 50% inhibitory concentration values were 0.82 nM for 17-AAG and 0.21 nM for MG132. Low concentrations of MG132 had strong synergistic inhibitory effects with low toxicity on HCV replicon cells.

Conclusions: The results of this study suggest that the different effects and synergistic actions of 17-AAG and MG132 could provide a new therapeutic approach to HCV infection.

Introduction

Infection by the hepatitis C virus (HCV) is a major public health problem, with 170 million chronically infected people worldwide [1,2]. Combined treatment with interferon-α and ribavirin induces sustained antiviral response in 80% of patients with HCV genotype 2 or 3 [3,4]. Chronic infection with HCV results in liver cirrhosis and can lead to hepatocellular carcinoma [5,6]. Although interferon-α plus ribavirin therapy is effective for approximately 50–80% of patients with HCV, the development of improved therapies and preventative vaccines is urgently needed [7].

Heat-shock protein 90 (Hsp90) exerts chaperone activity together with a number of cochaperones, playing an important role in the folding of at least 200 specific proteins of various signalling pathways and in the refolding of proteins that have been denatured by stress [8–11]. Hsp90 is considered to be of prime importance to the survival of cancer cells. The constitutive expression of Hsp90 is 2- to 10-fold higher in tumour cells compared with their normal counterparts, suggesting that Hsp90 is critically important for tumour cell growth and/or survival. A small molecule inhibitor of Hsp90, the benzoquinone ansamycin 17-AAG (17-allylamino-17-desmethoxy-geldanamycin; Figure 1A), exhibits antitumour activity in several human xenograft models, including colon, breast and prostate cancer [12–14]. The drug is currently completing multi-institution Phase I clinical trials, and Phase II trials are being planned.

The HCV non-structural protein 3 (NS3) forms a complex with Hsp90 [8,10,11] that is critical for HCV replication [15]. Treatment of the #50-1 HCV replicon cells with the Hsp90 inhibitor 17-AAG [8,16,17] suppresses HCV RNA replication and NS3 is the only HCV protein degraded in these cells [15]. This finding led us to suggest a crucial role for Hsp90–NS3 complexes in the HCV life cycle. By contrast, the proteasome is a large protein complex that also participates in protein degradation [18]. Among the 28 subunits of the 20S proteasome, the α-subunit 7 (PSMA7) is one of the α-ring subunits at the barrel centre of the proteasome complex. The 20S proteasome is activated upon

Figure 1. Schematic representation of the HCV replicon and the structures of 17-AAG and MG132

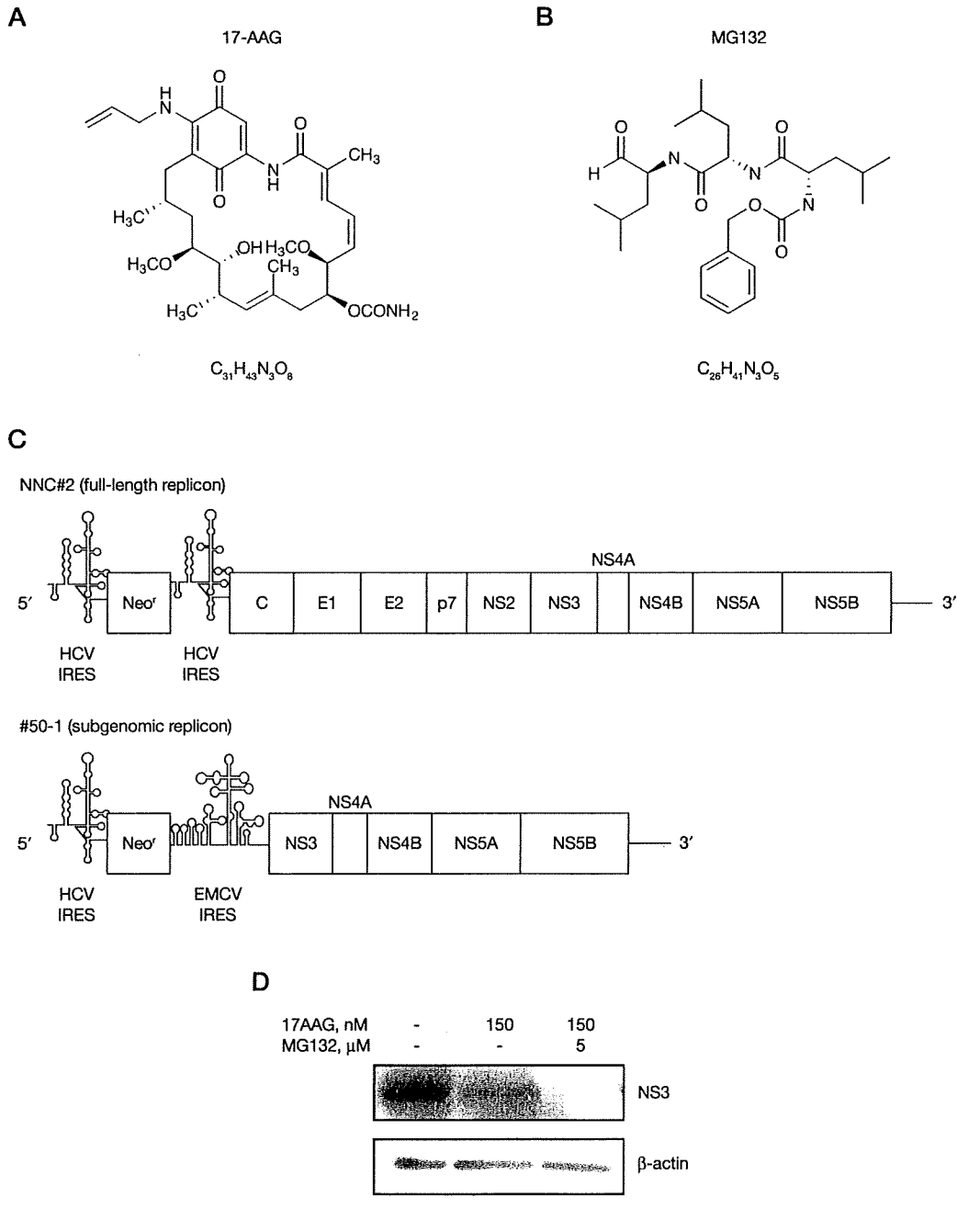

(A) Structure of the heat-shock protein 90 inhibitor 17-AAG. (B) Structure of the proteasome inhibitor MG132. (C) Structure of the hepatitis C virus (HCV) replicon RNAs comprising the HCV 5′-untranslated region, including the HCV internal ribosome entry site (IRES), the neomycin phosphotransferase gene (Neo′), the encephalomyocarditis virus (EMCV) IRES or the HCV IRES, and the coding region for HCV proteins NS3 to NS5B (in the HCV subgenomic replicon) or core protein to NS5B (in the HCV full-length replicon). (D) Effect of 17-AAG and MG132 on expression of the NS3 protein. β-Actin was used as a lysate control. The HCV full-length replicon (NNC#2 cells) was analysed by western blotting after 17-AAG treatment with or without MG132.

association with its regulatory protein complex, classified as PA700 (19S regulator) and PA28 (11S regulator) [18]. Ribozymes and small interference RNAs that specifically target the putative HCV cofactor PSMA7 inhibit HCV expression [19,20].

In the present study, we describe our findings of HCV combination therapy with the Hsp90 inhibitor 17-AAG and the proteasome inhibitor MG132 (Figure 1B). Combining these different inhibitors produced significant synergistic inhibitory effects on HCV replicons, indicating that the inhibitors might be useful as an efficient dual strategy of molecular HCV therapeutics.

Methods

Cell culture and reagents

The HCV replicon cell line #50-1 (NN/1b/SG) [21], which carries a subgenomic replicon, and NNC#2 (NN/1b/FL) [22], which carries a full genome replicon, were cultured in Dulbecco's modified Eagle's medium supplemented with 10% fetal bovine serum, non-essential amino acids, L-glutamine, penicillin–streptomycin, and 300–1,000 μg/ml G418 (Invitrogen, Carlsbad, CA, USA) at 37°C in 5% CO_2. Huh-7 cells were grown in Dulbecco's modified Eagle's medium supplemented with 10% fetal bovine serum, 100 U/ml penicillin and 100 mg/ml streptomycin. 17-AAG and MG132 were purchased from Sigma-Aldrich Chemical Co. (St Louis, MO, USA).

Real-time reverse transcriptase PCR analysis

HCV replicon cells were seeded at 1.5×10^5 cells in 24-well plates and cultured for 72 h. Total RNA was then isolated using Trizol (Invitrogen) according to the manufacturer's instructions. HCV RNA was quantified by real-time reverse transcriptase (RT)-PCR using an ABI 7700 sequence detector (Perkin-Elmer Applied Biosystems, Foster City, CA, USA), and the following primers and TaqMan probes located in the 5′-untranslated region: forward primer (nucleotides [nt] 130–146), 5′-CGGGAGAGCCATAGTGG-3′; reverse primer (nt 272–290), 5′-AGTACCACAAGGCCTTTCG-3′; and TaqMan probe (nt 148–168), 5′-CTGCGGAACCGGTGAGTACAC-3′ (all purchased from Applied Biosystems). The probe sequence was labelled with the reporter dye 6-carboxyflurorescein at the 5′-end and with the quencher dye TAMRA at the 3′-end [23].

Western blotting

NNC#2 cells were seeded at 1.5×10^5 cells in 24-well plates, treated with 17-AAG alone, MG132 alone, or combined 17-AAG and MG132, and cultured for 48 h. Western blotting analysis was performed using a previously described method [15]. The primary antibodies were monoclonal or polyclonal antibodies against PSMA7 (Abcam, Cambridge, MA, USA) and β-actine (SIGMA, Sigma Aldrich, St Louis, MO, USA). The anticore antibody was a kind gift from M Kohara (Tokyo Metropolitan Institute of Medical Science, Tokyo, Japan). Anti-NS3 antibody was a kind gift from Y Matsuura (Osaka University, Osaka, Japan).

Transfection and reporter assay

Huh-7 cells were seeded at 1.5×10^5 cells 24 h before transfection. Huh-7 cells were treated with MG132 (100 nM) following transfection with the plasmid DNA pHCV internal ribosome entry site (IRES) luciferase (luc) or pEMCV IRES luc using Lipofectamine 2000 (Invitrogen) according to the manufacturer's protocol. Luc activity was measured in the cell lysates using a luminometer (Berthold, Bad Wildbad, Germany).

MTS assay

HCV replicon cells were seeded in 96-well plates at 3×10^4 cells per well in a final culture volume of 100 μl for 72 h before adding increasing concentrations of 17-AAG and MG132. After incubation for 3 days, viable cell numbers were determined using the CellTitre 96® Aqueous non-radioactive cell proliferation assay (Promega Corp., Madison, WI, USA). The value of the background absorbance at 490 nm (A_{490}) of wells without cells was subtracted from the A_{490} value of wells with cells. The percentages of viable cells were then calculated using the following formula: (A_{490} 17-AAG-, MG132- or 17-AAG+MG132-treated cells/ A_{490} untreated cells)×100.

Drug synergism analysis

The effect of treatment of HCV replicon cells with 17-AAG and MG132, alone and in combination, was analysed by measuring HCV RNA with real-time PCR. The combination index (CI) for each combination of 17-AAG and MG132 treatment was calculated by the following formula using the 50% inhibitory concentration (IC_{50}): CI= IC_{50}(17-AAG combined)/IC_{50}(17-AAG alone) +IC_{50}(MG132 combined)/IC_{50}(MG132 alone). For such plots, the combined effects of the two drugs can be assessed as either additive (CI=1), synergistic (CI<1) or antagonistic (CI>1) [24].

Results

In a previous study, we examined the inhibitory effects of 17-AAG on HCV replication in an HCV replicon cell culture system. In HCV replicon cells treated with 17-AAG, HCV RNA replication was suppressed in a dose-dependent manner, and the only HCV protein degraded in these cells was NS3 [15]. To determine whether 17-AAG promoted the degradation of NS3,

Figure 2. Effect of proteasome inhibitor MG132 on HCV IRES activity

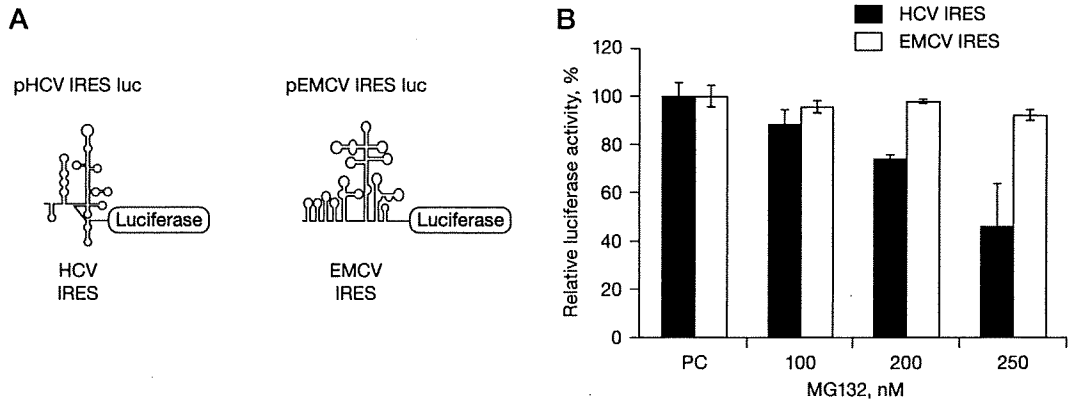

(A) Vector construct for hepatitis C virus (HCV) internal ribosome entry site (IRES)-mediated (pHCV IRES luc) or encephalomyocarditis virus (EMCV) IRES-mediated (pEMCV IRES luc) translation of firefly luciferase. (B) Huh-7 cells were transfected with pHCV IRES luc alone or pEMCV IRES luc alone (PC), or also treated with MG132 100, 200 and 250 nM. After 24 h, HCV IRES activity was determined by luciferase assay. Data are means ±SD of triplicate experiments.

we evaluated the effect of 17-AAG on #50-1 cells in which proteasomal degradation was also inhibited with the proteasome inhibitor MG132. Although 17-AAG treatment reduced NS3 levels in #50-1 cells, this NS3 degradation was completely blocked in the presence of MG132 [15]. In the present study, we used HCV full-length replicon NNC#2 cells (Figure 1C) [22] instead of the HCV subgenomic replicon #50-1 cells used in previous studies [15,21]. Treatment with 17-AAG decreased NS3 levels, but the presence of MG132 did not block the reduction in HCV NS3 (Figure 1D). Indeed, MG132 in combination with 17-AAG induced the complete disappearance of the NS3 (Figure 1D), suggesting that the reduction of HCV NS3 induced by treatment with the proteasome inhibitor MG132 was dependent on the HCV IRES. NNC#2 and #50-1 cells have different virus IRESs, known as the HCV IRES [25–27] and the encephalomyocarditis virus (EMCV) IRES [28], and HCV IRES-mediated translation is induced by PSMA7 [29]. The PSMA7 activity is blocked by MG132 [30]. Similar effects were observed when PSMA7-directed ribozyme or small interfering RNAs inhibited HCV replication [19,20].

We examined the effects of combination therapy with 17-AAG and MG132 on HCV. To evaluate the MG132-mediated effect on HCV IRES activity, Huh-7 cells were treated with MG132 (100, 200 and 250 nM) and then transfected with pHCV IRES luc or pEMCV IRES luc (Figure 2A). MG132 inhibited luc activity of HCV IRES in dose-dependent manner, but did not inhibit translation derived from EMCV IRES (Figure 2B), indicating a preferential effect of MG132 on HCV IRES activity [19]. NNC#2 cells were then treated with 17-AAG or MG132 for 3 days. HCV RNA was quantified by real-time RT-PCR using an ABI 7500 Fast (Perkin-Elmer, Applied Biosystems). Dose-dependent cytotoxicity was not observed upon application of MG132 and/or 17-AAG (99% at concentrations ranging between 5 and 25 nM; Figure 3A), but was observed at MG132 concentrations of 10 μM (data not shown). Cells treated with increasing doses of 17-AAG or MG132 showed reduced levels of HCV RNA (Figure 3B). Low concentrations (1 nM) of MG132 had inhibitory effects similar to those of 15 nM 17-AAG (Figure 3B). In NNC#2 cells treated with 5 nM MG132, HCV RNA replication was suppressed by 85%, and this effect was dose-dependent (Figure 3B). The IC_{50} values were 0.82 nM for 17-AAG and 0.21 nM for MG132 (Table 1 and Figure 3B).

We also investigated combination therapy with 17-AAG and MG132 on HCV in NNC#2 cells. In combination with 5 nM, 15 nM or 25 nM of 17-AAG, 0.5 nM, 1 nM or 5 nM of MG132 was applied to NNC#2 cells, respectively. The combination of 5 nM 17-AAG and 1 nM MG132 suppressed HCV RNA replication by 90% in the NNC#2 cells (Figure 3B). The CI was 0.42, demonstrating that 17-AAG and MG132 had synergistic inhibitory effects on HCV replicon cells (Table 1). The combination of 17-AAG with MG132 inhibited HCV RNA replication with an approximately 2.5-fold reduction in the dose (Table 1). To determine the effects of 17-AAG and MG132 on the expression of core and PSMA7 proteins, NNC#2 cells were treated

Figure 3. MG132 and 17-AAG inhibition of HCV RNA replication in HCV replicon cells

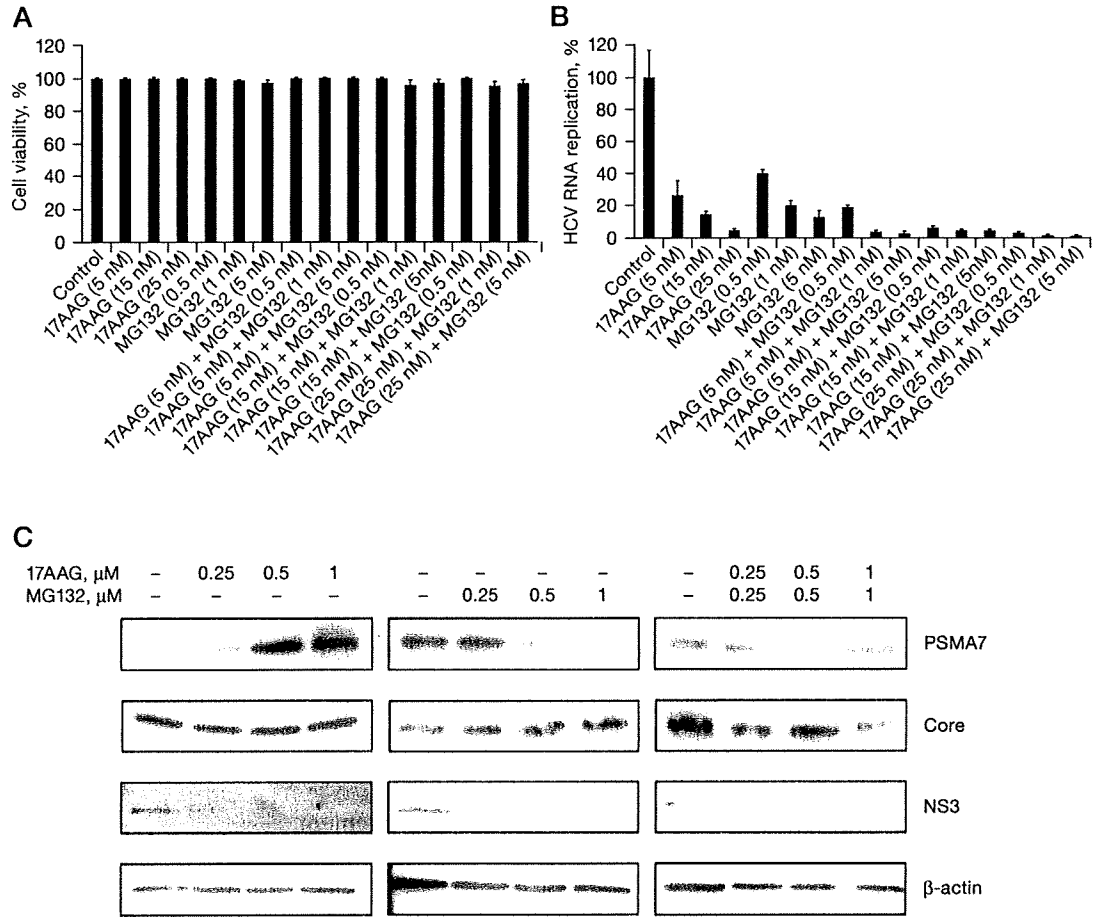

(A) Cytotoxic effects of 17-AAG and MG132, singly or in combination, on NNC#2 cells, shown as the percentage reduction of the number of viable cells assessed by MTS assay. Data are means ±SD of triplicate experiments. (B) Inhibition of hepatitis C virus (HCV) replication by 17-AAG and MG132, singly or in combination, in NNC#2 cells. Measurement of HCV replication by real-time reverse transcriptase PCR. Data are means ±SD of triplicate experiments. (C) Effect of 17-AAG and MG132 on the expression of core, non-structural protein 3 (NS3) and the proteasome α-subunit 7 (PSMA7) protein. The core, NS3 and PSMA7 protein were analysed by western blotting after treatment of NNC#2 cells with various concentrations of 17-AAG or MG132, alone or in combination. β-Actin was used as a lysate control.

with various concentrations of 17-AAG or MG132 alone, and 17-AAG plus MG132 at day 2. Treatment with 17-AAG alone increased the expression of PSMA7, but did not reduce core protein expression. By contrast, treatment with MG132 alone reduced the expression of PSMA7, but not the core protein (Figure 3C), whereas expression of NS3 was reduced by treatment with 17-AAG or MG132 alone, and 17-AAG plus MG132. This result was consistent with our previous findings that NS3 levels were reduced in NNC#2 cells treated with 17-AAG for 3 days, but that core protein

Table 1. Combination index and dose reduction in inhibition of hepatitis C virus RNA replication by combining 17-AAG with MG132

Drug	IC_{50}, nM		Fold dose reduction[a]
	Alone	In combination	
17-AAG	0.82	0.33	2.52
MG132	0.21	0.01	21.00

The combination index for 17-AAG and MG132 was 0.42. [a]Dose reduction is the 50% inhibitory concentration [IC_{50}] of the drug in combination. Each sample was tested in triplicate and the mean values are presented

was detected for up to 6 days [15]. Other researchers, however, have reported that MG132 blocks the degradation of HCV core protein [31]. Interestingly, combined treatment with MG132 and 17-AAG reduced the expression of both the core and PSMA7 proteins in NNC#2 cells (Figure 3C). These results suggest that MG132 and 17-AAG are potent anti-HCV agents, and are more effective in combination therapy than as single monotherapeutic agents.

Discussion

HCV is a major cause of chronic liver disease. The results of the present study indicate that the individual effects of the Hsp90 inhibitor 17-AAG on HCV replicon cells and the synergistic action of the proteasome inhibitor MG132 might account for the improved clinical response to combination therapy. We previously reported a new and effective strategy for inhibiting HCV replication using 17-AAG to inhibit Hsp90 [15]. The mechanism by which 17-AAG so effectively suppresses HCV replication is the destabilization of NS3, which disrupts the Hsp90 chaperone complex. A previous study demonstrated that HCV NS3 degradation is greatly increased by treatment of HCV subgenomic replicon #50-1 cells with 17-AAG, but this degradation is completely blocked in the presence of the proteasome inhibitor MG132 [15]. By contrast, in the present study we used HCV full-length replicon NNC#2 cells in place of HCV subgenomic replicon #50-1 cells used in previous studies [15]. The resulting 17-AAG treatment reduced NS3 levels, but MG132 treatment of NNC#2 cells did not block the degradation of HCV NS3 (Figure 1D). This blocking efficiency significantly influenced the different activities of the virus IRES (that is, HCV IRES and EMCV IRES) [25–28]. In our assays, when Huh-7 cells exposed to MG132 were transfected with pHCV IRES luc or pEMCV IRES luc, HCV IRES activity was inhibited, but EMCV IRES was not (Figure 2B). Apcher *et al.* [29] reported that HCV IRES-mediated translation can be induced by PSMA7. The proteasome inhibitor MG132 inhibits PSMA7 activity. These findings demonstrate that HCV IRES activity is also reduced by MG132. By contrast, degradation of NS3 by 17-AAG is dependent on the proteasome system [15].

The present study demonstrated that NNC#2 cells containing a full HCV genome replicon treated with 17-AAG or MG132 for 3 days did not show dose-dependent cytotoxicity (Figure 3A), but 10 μM MG132 was cytotoxic (data not shown). As shown in the present study, the IC_{50} values were 0.82 nM for 17-AAG and 0.21 nM for MG132 (Table 1 and Figure 3B). These data provide evidence that a dual treatment strategy with 17-AAG and MG132 inhibits HCV replication. The combination of 5 nM 17-AAG and 1 nM MG132 suppressed HCV RNA replication by 90% in NNC#2 HCV replicon cells (Figure 3B). The two drugs, 17-AAG and MG132, had synergistic inhibitory effects on HCV replicon (Table 1). Importantly, the combined use of these different groups of inhibitors showed strong synergistic inhibitory effects on HCV replication, indicating that combining these inhibitors might be a useful and efficient strategy for anti-HCV chemotherapy.

Given the absence of a single effective and proven antiviral agent against HCV, the combination of 17-AAG with agents that possess potential antiviral effects will continue to dominate novel therapeutic approaches. The present study demonstrated a strong synergistic effect of 17-AAG and MG132 on intracellular HCV replication, and these effects are attributable to the direct and specific inhibition of viral replication. Our results indicate that antiviral treatment with 17-AAG might be improved by combining 17-AAG with MG132, and that this combination therapy might be a feasible strategy for the treatment of HCV infection. Modifications of these inhibitors might also result in the development of more effective antiviral compounds.

Acknowledgements

We are grateful to M Sato and Y Katumura for excellent technical assistance. This work was supported by a Grant-in-Aid for HCV research from the Ministry of Health, Labor, and Welfare of Japan, and by a Grant-in-Aid for High Technology Research from the Ministry of Education, Science, Sports, and Culture of Japan.

Disclosure statement

The authors declare no competing interests.

References

1. Alter HJ, Purcell RH, Shin JW, *et al.* Detection of antibody to hepatitis C virus in prospectively followed transfusion recipients with acute and chronic non-A, non-B hepatitis. *N Engl J Med* 1989; 321:1494–1500.
2. Choo QL, Kuo G, Weiner AJ, Overby LR, Bradley DW, Houghton M. Isolation of a cDNA clone derived from a blood-borne non-A, non-B viral hepatitis genome. *Science* 1989; 244:359–362.
3. Chevaliez S, Pawlotsky JM. Hepatitis C virus: virology, diagnosis and management of antiviral therapy. *World J Gastroenterol* 2007; 13:2461–2466.
4. Witthöft T. Review of consensus interferon in the treatment of chronic hepatitis C. *Biologics* 2008; 2:635–643.
5. Saito I, Miyamuram T, Ohbayashi A, *et al.* Hepatitis C virus infection is associated with the development of hepatocellular carcinoma. *Proc Natl Acad Sci U S A* 1990; 87:6547–6549.
6. Seeff LB. Natural history of hepatitis C. *Hepatology* 1997; 26:21S–28S.
7. Reddy KR, Wright TL, Pockros PJ, *et al.* Efficacy and safety of pegylated (40-kd) interferon alpha-2a compared with interferon alpha-2a in noncirrhotic patients with chronic hepatitis C. *Hepatology* 2001; 33:433–438.

8. McClellan AJ, Frydaman J. Molecular chaperones and the art of recognizing a lost cause. *Nat Cell Biol* 2001; **3**:E51–E53.
9. Pratt WB, Toft DO. Regulation of signalling protein function and trafficking by the hsp90/hsp70-based chaperone machinery. *Exp Biol Med (Maywood)* 2003; **228**:111–133.
10. Picard D. Heat-shock protein 90, a chaperone for folding and regulation. *Cell Mol Life Sci* 2002; **59**:1640–1648.
11. Wegele H, Muller L, Buchner J. Hsp70 and Hsp90–α relay team for protein folding. *Rev Physiol Biochem Pharmacol* 2004; **151**:1–44.
12. Basso AD, Solit DB, Munster PN, Rosen N. Ansamycin antibiotics inhibit Akt activation and cyclin D expression in breast cancer cells that overexpress HER2. *Oncogene* 2002; **21**:1159–1166.
13. Kelland LR, Sharp SY, Rogers PM, Myers TG, Workman P. DT-diaphorase expression and tumor cell sensitivity to 17-allylamino, 17-demethoxygeldanamycin, an inhibitor of heat shock protein 90. *J Natl Cancer Inst* 1999; **91**:1940–1949.
14. Solit DB, Zheng FF, Drobnjak M, *et al.* 17-allylamino-17-demthoxygeldanamycin induces the degradation of androgen receptor and HER-2/neu and inhibits the growth of prostate cancer xenografts. *Clin Cancer Res* 2002; **8**:986–993.
15. Ujino S, Yamaguchi S, Shimotohno K, Takaku H. Heat-shock protein 90 is essential for stabilization of the hepatitis C virus nonstructural protein NS3. *J Biol Chem* 2009; **284**:6841–6846.
16. Supko JG, Hickman RL, Grever MR, Malspeis L. Preclinical pharmacologic evaluation of geldanamycin as an antitumor agent. *Cancer Chemother Pharmacol* 1995; **36**:305–315.
17. Grenert JP, Sullivan WP, Fadden P, *et al.* The amino-terminal domain of heat shock protein 90 (hsp90) that binds geldanamycin is an ATP/ADP switch domain that regulates hsp90 conformation. *J Biol Chem* 1997; **272**:23843–23850.
18. Tanaka K. Molecular biology of the proteasome. *Biochem Biophys Res Commun* 1998; **247**:537–541.
19. Krüger M, Beger C, Welch PJ, Barber JR, Manns MP, Wong-Staal F. Involvement of proteasome α-subunit PSMA7 in hepatitis C virus internal ribosome entry site-mediated translation. *Mol Cell Biol* 2001; **21**:8357–8364.
20. Korf M, Jarczak D, Beger C, Manns MP, Krüger M. Inhibition of hepatitis C virus translation and subgenomic replication by siRNAs directed against highly conserved HCV sequence and cellular HCV cofactors. *J Hepatol* 2005; **43**:225–234.
21. Ishii N, Watashi K, Hishiki T, *et al.* Diverse effects of cyclosporine on hepatitis C virus strain replication. *J Virol* 2006; **80**:4510–4520.
22. Kishine H, Sugiyama K, Hijikata M, *et al.* Subgenomic replicon derived from a cell line infected with the hepatitis C virus. *Biochem Biophys Res Commun* 2002; **293**:993–999.
23. Takeuchi T, Katsume A, Tanaka T, *et al.* Real-time detection system for quantification of hepatitis C virus genome. *Gastroenterology* 1999; **116**:636–642.
24. Tanabe Y, Sakamoto N, Enomoto N, *et al.* Synergistic inhibition of intracellular hepatitis C virus replication by combination of ribavirin and interferon-α. *J Infect Dis* 2004; **189**:1129–1139.
25. Tsukiyama-Kohara K, Iizuka N, Kohara M, Nomoto A. Internal ribosome entry site within hepatitis C virus RNA. *J Virol* 1992; **66**:1476–1483.
26. Hellen CU, Pestova TV. Translation of hepatitis C virus RNA. *J Viral Hepat* 1999; **6**:79–87.
27. Honda M, Beard MR, Ping LH, Lemon SM. A phylogenetically conserved stem-loop structure at the *5′* border of the internal ribosome entry site of hepatitis C virus is required for cap-independent viral translation. *J Virol* 1999; **73**:1165–1174.
28. Hellen CU, Wimmer E. Translation of encephalomycarditis virus RNA by internal ribosomal entry. *Curr Top Microbiol Immunol* 1995; **203**:31–63.
29. Apcher GS, Maitland J, Dawson S, Sheppard P, Mayer RJ. The alpha4 and alpha7 subunits and assembly of the 20S proteasome. *FEBS Lett* 2004; **569**:211–216.
30. Meiners S, Heyken D, Weller A, *et al.* Inhibition of proteasome activity induces concerted expression of proteasome genes and *de novo* formation of Mammalian proteasomes. *J Biol Chem* 2003; **278**:21517–21525.
31. Moriishi K, Okabayashi T, Nakai K, *et al.* Proteasome activator PA28gamma-dependent nuclear retention and degradation of hepatitis C virus core protein. *J Virol* 2003; **77**:10237–10249.

Received 27 July 2009, accepted 19 September 2009